Solar Energy Materials & Solar Cells 287 (2025) 113622

Contents lists available at ScienceDirect

Solar Energy Materials and Solar Cells

journal homepage: www.elsevier.com/locate/solmat

Enhancing tubular solar still productivity: A novel rotational absorber, ultrasonic atomizer, and hygroscopic fabric integration

Fuhaid Alshammari [a,*], Nasser Alanazi [b], Mamdouh Alshammari [a], Ammar H. Elsheikh [c], Fadl A. Essa [d,e,**]

[a] Mechanical Engineering Department, Engineering College, University of Ha'il, Ha'il, 2440, Saudi Arabia
[b] Civil Engineering Department, College of Engineering, University of Hail, Hail, 2440, Saudi Arabia
[c] Department of Production Engineering and Mechanical Design, Tanta University, Tanta, 31527, Egypt
[d] Mechanical Engineering Department, Faculty of Engineering, Kafrelsheikh University, Kafrelsheikh, 33516, Egypt
[e] Pharos University in Alexandria, Canal El Mahmoudia Street, Beside Green Plaza Complex, 21648, Alexandria, Egypt

ARTICLE INFO

Keywords:
Solar desalination
Tubular solar distiller
Wick materials
Rotating absorber
Activation and deactivation periods

ABSTRACT

Freshwater scarcity is a growing global challenge, particularly in regions with abundant solar energy but limited access to clean water. Conventional solar stills offer a sustainable solution for freshwater production but suffer from low productivity and efficiency, limiting their practical application. This study addresses these limitations by introducing a novel tubular solar still design with operational enhancements aimed at significantly improving freshwater productivity and thermal efficiency. Key innovations include a centrally suspended rectangular absorber plate with an adjustable rotational mechanism, microcontroller-regulated rotational velocity control, and an ultrasonic atomizer at the still's apex to intermittently disperse water droplets for enhanced evaporation. Hygroscopic burlap fabrics (cotton and jute) were layered on the absorber to amplify surface evaporation. Comprehensive experiments optimized rotational speeds (0–2 rpm) and atomizer duty cycles (fixed 1-min activation with varied deactivation intervals: 2–10 min) to maximize freshwater yield through parametric refinement of rotational dynamics and misting cycles. Key parameters contributing to the system's performance include thermal efficiency, freshwater yield, cost-effectiveness, environmental impact, and durability. Experimental results demonstrated that the modified tubular solar distiller (MTSD) with a rotational suspended absorber increased freshwater yield by 18 % compared to the reference system (RTSD). Jute cloth outperformed cotton, achieving a 90 % productivity improvement versus 82 % for cotton. Optimal performance occurred under conditions combining jute cloth, 1 rpm rotation, and an atomizer duty cycle of 1 min ON/8 min OFF, yielding a 97 % productivity increase (6795 mL/m^2 for MTSD versus 3450 mL/m^2 for RTSD) and 49 % thermal efficiency, significantly surpassing the RTSD baseline. Life-cycle cost analysis demonstrated a 52 % reduction in unit production costs for the MTSD configuration with jute-based rotational operation (1 rpm), achieving 0.013/L, compared to 0.025/L for RTSD. These results underscore the efficacy of the design enhancements in maximizing solar still productivity, offering a promising solution to address freshwater scarcity in resource-limited settings.

Abbreviations and symbols

Symbol	Definition
A	Absorber area
AMC	Yearly maintenance costs
ASV	Yearly salvage value
CO_2	Carbon dioxide
CPL	Cost per liter
CRF	Capital recovery factor
E_{in}	Embodied energy of the system's components
E_{out}	Annual energy output
F	Fixed costs

(continued on next column)
(continued)
(continued on next page)

* Corresponding author. Mechanical Engineering Department, Engineering College, University of Ha'il, Ha'il, 2440, Saudi Arabia.
** Corresponding author. Mechanical Engineering Department, Faculty of Engineering, Kafrelsheikh University, Kafrelsheikh 33516, Egypt.
E-mail addresses: Fu.alshammari@uoh.edu.sa (F. Alshammari), fadlessa@eng.kfs.edu.eg, eng.fadl.mech@gmail.com (F.A. Essa).

https://doi.org/10.1016/j.solmat.2025.113622
Received 9 February 2025; Received in revised form 24 March 2025; Accepted 30 March 2025
Available online 7 April 2025

(*continued*)

Symbol	Definition
FAC	Fixed annual cost
G	Solar irradiance
GHG	Greenhouse gas
h_{fg}	Latent heat of vaporization
i	Interest rate
LCAs	Life cycle assessments
m	Mass of distillate
M	Yearly distillate
MTSD	Modified tubular solar distiller
n	Lifespan
N	Working a year
RSS	Root-sum-square
RTSD	Reference tubular solar distiller
S	Salvage value
SFF	Sinking fund factor
t	Time
TAC	Total annual cost
V	Bottle volume measurement
Y	Distillate yield
Z'	Environmental performance indicator
δ	Uncertainty
η	Thermal efficiency
$\phi(CO_2)$	Net co_2 reduction

1. Introduction

Human survival is inextricably linked to freshwater resources, yet readily accessible freshwater constitutes less than 1 % of the Earth's total water supply [1,2]. The escalating demands of urbanization and industrial expansion have exacerbated the global freshwater crisis, elevating it to a critical challenge for human societies [3–5]. Projections indicate that by 2040, a significant number of countries, potentially as many as 33, will face severe freshwater shortages [6,7]. Desalination technology currently presents a crucial avenue for mitigating freshwater scarcity [8–10]. While established desalination methods like multi-effect distillation offer potential solutions [11–14], their inherent complication, power consumption, and extravagantly operational costs often make them less attractive over other cheap distillers [15–17]. Nevertheless, the present efficiency levels of existing solar still designs remain relatively low [18–20], underscoring the critical need for ongoing research and development to enhance their performance [21,22].

Conventional solar stills, in spite of their merits of cost-effectiveness, ease of operation, and environmental friendliness, exhibit limitations in their efficiency [23,24]. Thermal losses via the glazing covering significantly impacts the performance, typically yielding around 3 L of freshwater per day with efficacy ~30 % [25–28]. This efficacy varies considerably based on design and location [29–31]. To address these limitations and enhance the performance of conventional solar stills, researchers have explored a range of designable adjustments [32–36]. One outstanding approach takes growing the vaporization surface through novel configurations [37–39]. This includes incorporating discs [40] and balls [41,42] within the still to disrupt surface tension and maximize sun exposure, as well as employing trays tray [43], dish-shaped [44,45], and standing [46,47] configurations to heighten the vaporization surface of the distillate. Furthermore, scholars studied the operation of stepped absorbers [48–50] to expand the water surface area for evaporation, wicks [51] and nanomaterials [52,53] to leverage capillary action for enhanced evaporation, and drum [54,55] cylinders to accelerate the vaporization rate. Additionally, studies have explored the use of tubular [56–58], floating [59], semispherical [60–62], inverted [63], and pyramidal [64–67] configurations to enhance irradiance absorption. The goal of these improvements to the structure is to improve evaporating speeds, which will raise the amount of freshwater produced.

Recent research efforts have prioritized enhancing solar thermal absorption and thermal retention within distillation basins through multifaceted engineering interventions [68,69]. Notable advancements include: Geometric optimization of basin liners [70,71] to maximize irradiance exposure; Nano-enhanced coatings [72] and nanofluids [53] to amplify conductive heat transfer at material interfaces; Reflective surface geometries [73–75] designed to intensify solar flux density on the evaporation zone; evacuated tube collectors [76–79] to provide warm water to the distiller; Porous sandy bed substrates [80] to augment capillary-driven water distribution; and Thermal buffering via phase change materials (PCMs) [56,81,82] to store latent heat during insolation peaks for nocturnal utilization. These synergistic interventions collectively target multi-domain performance enhancement in freshwater yield and thermodynamic efficiency. Furthermore, emerging technical approaches such as nanostructured composites [83,84] for selective radiation absorption, dynamic rotational components [35,85] to regulate interfacial temperature gradients, and dedicated condenser architectures [86,87] with optimized vapor-to-liquid pathways demonstrate significant promise in addressing critical challenges in vapor condensation management and parasitic thermal losses. Moreover, introducing water heater via utilizing vacuum tubes to the solar distiller provided improved performance [88]. The distillate was reported as 12.4 kg a day. While Singh and Samsher [89] stated that the integration of evacuated tubes with a number of 4 was the optimal condition for providing the best performance of solar still.

Tubular solar stills (TSS) have consistently outperformed conventional solar stills (CSS) in terms of efficiency and freshwater yield [90]. Recent advancements in thermal solar still (TSS) optimization have emphasized hybrid system integration and advanced material engineering. Empirical evidence highlights the efficacy of coupling TSS with solar concentration technologies: Arunkumar et al. [91] demonstrated a 33.7 % increase in freshwater yield through the synergistic integration of a compound parabolic concentrator (CPC), attributing this enhancement to intensified solar flux density. Parallel innovations in thermal energy storage have proven impactful, with paraffin wax—a PCM—embedded in TSS configurations yielding an 8.4 % productivity enhancement [92], likely due to improved diurnal latent heat regulation. Chaichan and Kazem [93] introduced a concentrating solar dish to heat up a paraffin wax as a PCM for solar desalination unit. The system distillate was augmented by 307.54 %.

Elashmawy's experimental study [94] further validated the role of thermal mass augmentation, where gravel beds incorporated into the TSS basin improved productivity and thermal efficiency by 14.2 % and 13.9 %, respectively, by extending interfacial evaporation duration. The most striking progress, however, emerged from nanocomposite-enhanced systems: Kabeel et al. [56] achieved 41.3 % higher daily yield and 116.5 % efficiency improvement by hybridizing paraffin wax with graphene oxide nanoparticles, a design that concurrently optimizes thermal conductivity and phase transition kinetics. These findings collectively underscore the transformative potential of multi-physics approaches in TSS performance amplification.

Recent experimental investigations have demonstrated the efficacy of mechanical augmentation in solar still systems, particularly through the implementation of rotating drum mechanisms, which markedly improve freshwater productivity. Malaeb et al. [90] documented a 250 % enhancement in distillate output through dynamic rotational interfacing, a phenomenon attributed to optimized interfacial turbulence and heat transfer coefficients. Extending this paradigm, Abdullah et al. [54] systematically evaluated the hydrodynamic influence of drum angular velocity on evaporation kinetics, achieving unprecedented freshwater yield amplification (350 %) through precise regulation of rotational parameters.

Diverging from rotational methods, Al-Nimr [95] developed a hybrid configuration combining finned thermal storage units with parabolic solar concentrators, achieving a daily output of 3.0 kg/m^2 at 33.8 % thermodynamic efficiency through synergistic radiant flux

concentration and thermal inertia modulation. Concurrently, Arunkumar and Kabeel [92] pioneered a dual-enhanced TSS architecture integrating compound parabolic concentrators (CPCs) with PCM matrices, demonstrating 41.3 % productivity gains over conventional designs through concurrent optimization of optical capture and latent heat utilization. These studies collectively highlight the transformative potential of multifunctional system integration in solar desalination technology.

This study aims to enhance the productivity of a tubular solar distiller through innovative design modifications and operational optimizations. The key objectives are: (1) to integrate a centrally suspended rectangular absorber plate with an adjustable tilt mechanism for improved solar energy absorption; (2) to implement a microcontroller-based system for regulating the rotational velocity of the absorber plate; and (3) to incorporate an ultrasonic atomizer and hygroscopic burlap fabric to augment evaporative efficiency. Comparative analyses were conducted using two burlap materials (cotton and jute), and the system's performance was evaluated across varying rotational speeds (0, 0.5, 1, 1.5, and 2 rpm) and atomizer duty cycles (ON time = 1 min, OFF times = 2, 4, 6, 8, and 10 min). Besides, economic and environmental studies were conducted to obtain the reliability of the proposed system. The overarching goal is to maximize freshwater yield by systematically optimizing these parameters, thereby advancing the practical applicability of solar distillation systems.

2. Materials & method

2.1. Fabrication and assembly of the test rig

The experimental investigation employed a comparative configuration featuring two tubular solar distillation units, accompanied by a saline water reservoir and supporting instrumentation (Fig. 1). The modified tubular solar distiller (MTSD) integrated the proposed design enhancements, while the reference tubular solar distiller (RTSD) retained a conventional configuration as the control. A rectangular saline water reservoir (0.5 m × 0.5 m × 1 m) supplied both systems with feedwater via gravity-driven flow. Both distillers were fabricated from 0.015 m thick galvanized steel sheets, with identical cylindrical geometries (0.8 m diameter × 1 m length) and a projected footprint of 0.8 m^2. To maximize solar irradiance absorption, the external surfaces of both units were coated with a matte black acrylic polymer. A transparent glass cover (0.8 m diameter × 1 m length × 0.04 m thickness) encapsulated each distiller, forming a sealed evaporation-condensation chamber. Condensed freshwater was collected through bottom-mounted drainage ports into calibrated volumetric flasks for hourly yield quantification.

The RTSD and the MTSD, shown in Fig. 2, were identical in terms of size and composition. It nevertheless managed to include a number of changes. A rectangular absorber plate was suspended centrally within the tubular structure, secured by a dual-screw adjustable mechanism to allow controlled tilting and rotation. Also, an ultrasonic atomizer, operating at 6 W, was installed at the apex of the still to intermittently spray fine water droplets onto the absorber surface, enhancing evaporation rates. Besides, the absorber plate was layered with hygroscopic burlap fabric (cotton and jute) to increase surface area and improve capillary action for water retention. While these natural fibers offer excellent hygroscopic properties, their durability under prolonged salt-water exposure must be considered. Experimental validation using accelerated aging tests (ASTM D543-14) revealed a weight loss of 8 % and a 25 % reduction in tensile strength after 500 h of exposure to a 3.5 % saline solution. Based on these findings and supporting literature [96, 97], It can be estimated that the operational lifetime of untreated burlap

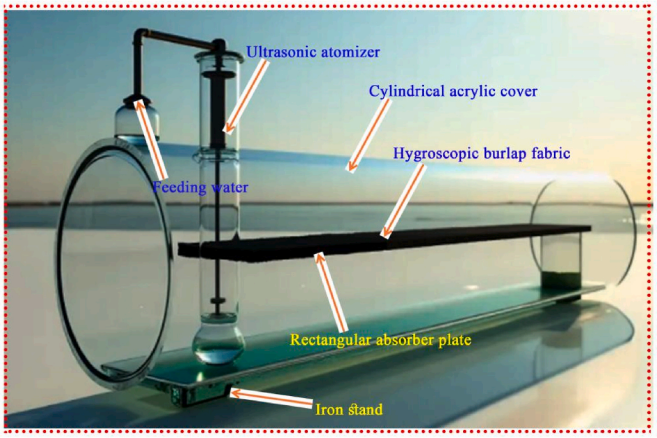

Fig. 2. 3-D drawing of MTSD.

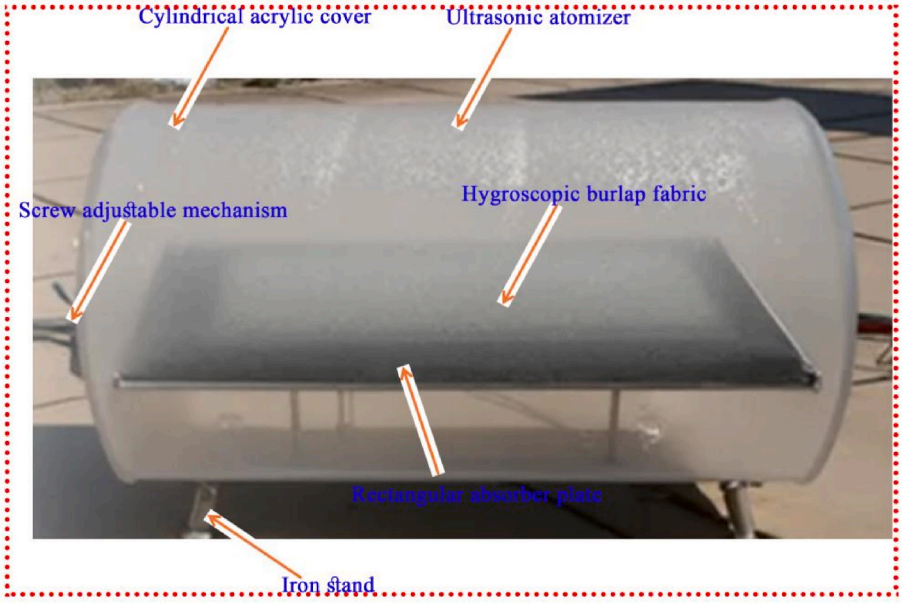

Fig. 1. Photograph of the MTSD.

fabric to be 6–12 months in high-salinity environments. To enhance durability, surface treatments such as acetylation or polyurethane coating are recommended, which can reduce strength loss to less than 10 % over 6 months [98]. Periodic replacement of the fabric every 6 months is advised to ensure sustained performance. Moreover, a microcontroller-based electrical circuit, has a power consumption of 10–15 mA with 9V battery, was integrated to regulate the rotational speed of the absorber plate, enabling precise control and optimization. Also, it can be concluded that the power consumption by the atomizer and microcontroller was too small as compared to the performance improvement obtained in section 3. The assembly process involved careful alignment of components to ensure uniform solar exposure and efficient vapor condensation. Both stills were mounted on a rigid frame to maintain stability during operation.

2.2. Experimental procedures

The experimental investigation was conducted in a controlled outdoor environment to assess the operation of the MTSD under various operational considerations. Since the experiments were conducted outdoors, ensuring the reliability and validity of the results required that all tests be performed under weather conditions that were as consistent and comparable as possible. To further enhance the accuracy of the findings, each experiment was repeated three times, and the average values were calculated to ensure robust and reliable data analysis. Below is a flowchart, shown in Fig. 3, summarizing the experimental procedures. The flowchart is structured to clearly depict the sequence of experiments and highlight key parameters investigated in each step. The following sequential procedures were adopted:

1. The first stage of experimentations was to evaluate the performance of MTSD with suspended absorber. The MTSD was tested with the suspended absorber plate in a stationary position (0 rpm) to establish a baseline for comparison with the RTSD. Key performance metrics, including freshwater yield, evaporation rate, and thermal efficiency, were recorded.
2. The second stage of experimentations was to test the effect of wick material on MTSD performance. The absorber plate was covered with two types of burlap fabric (cotton and jute) to study the influence of wick material on evaporation and condensation rates. Each material was tested under identical solar conditions, and the distillate output was measured to determine the optimal wick type.
3. The third stage of tests was to make an optimization of absorber plate rotational speed. The rotational speed of the absorber plate was varied (0, 0.5, 1, 1.5, and 2 rpm) to investigate its impact on system performance. The microcontroller-based control system ensured precise speed regulation, and the corresponding freshwater yield was recorded for each setting.
4. The final stage of tests was to conduct an atomizer duty cycle optimization. The atomizer's operational cycle was systematically optimized by maintaining a fixed activation interval (ON time = 1 min) while testing deactivation periods of 2, 4, 6, 8, and 10 min. This study aimed to identify the optimal misting frequency for maximizing evaporation and freshwater production.

2.3. Measuring tools and instrumentation

To ensure accurate data collection and performance evaluation of the Reference Tubular Solar Still (RTSD) and Modified Tubular Solar Distiller (MTSD), the following measuring tools and instruments were employed:

- Pyranometer: A calibrated pyranometer (Uncertainty: ±1.5 % of the measured value) was used to measure global solar irradiance (W/m^2) incident on the solar stills. The device was positioned parallel to the still's surface to ensure accurate readings.
- K-Type thermocouples: Thermocouples (Uncertainty: ±0.5 °C) with a temperature range of −50 °C–500 °C were installed at key locations, including the absorber plate, water surface, glass cover, and ambient environment. Also, a high-precision data logger was used to record temperature readings at regular intervals (e.g., every 5 min).
- Graduated cylinder: A calibrated graduated cylinder (Uncertainty: ±0.5 mL) with a resolution of 1 mL was used to measure the volume of freshwater collected. Besides, a precision digital scale (Uncertainty: ±0.02 g) was employed to weigh the distillate for cross-verification.
- Tachometer: A non-contact digital tachometer (Uncertainty: ±0.1 rpm) was used to measure the rotational speed of the absorber plate (in rpm).
- Anemometer: A cup-type anemometer (Uncertainty: ±0.2 m/s) was used to measure wind speed (m/s) near the test rig, as it can affect convective heat losses.
- Flow meter: A low-flow digital flow meter (Uncertainty: ±0.1 mL/min) was used to measure the water flow rate to the atomizer (mL/min).

Specifications of the equipment employed for the tests are shown in Table 1. The generated errors are used to quantify the accuracy of the measurements made throughout the course of the study.

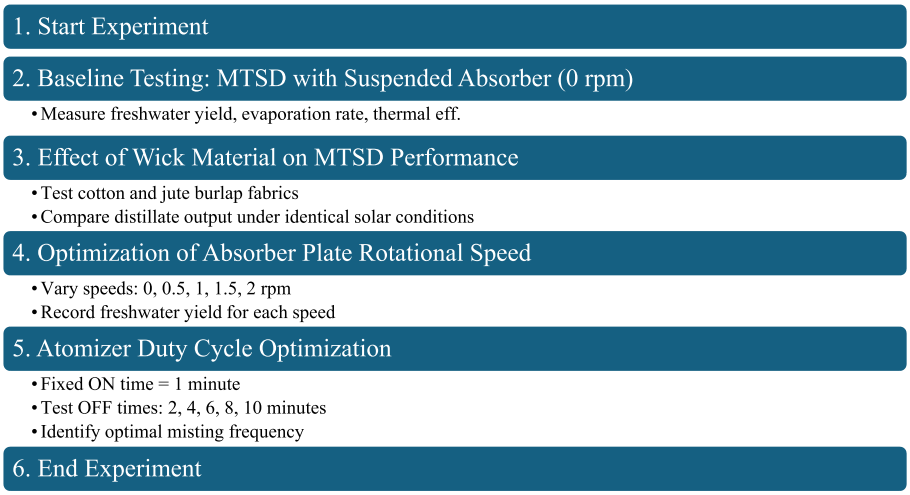

Fig. 3. Flowchart summarizing the experimental procedures.

Table 1
Summary of uncertainty and range values and parameters.

Parameter	Instrument	Unit	Range	Uncertainty
Solar Irradiance	Pyranometer	W/m^2	0 to 2000	±1.5 %
Temperature	Thermocouple	°C	−50 to 250	±0.5 °C
Distillate Volume	Graduated cylinder	mL	0 to 2500	±0.5 mL
Distillate Mass	Digital scale	g	0 to 10000	±0.02 g
Rotational Speed	Tachometer	rpm	0 to 50	±0.1 rpm
Wind Speed	Anemometer	m/s	0.1 to 30	±0.2 m/s
Atomizer Flow Rate	Flow meter	mL/min	0 to 10000	±0.1 mL/min

2.4. Error analysis and uncertainty quantification

To ensure the reliability of experimental results, a comprehensive error analysis was conducted. The following steps outline the methodology for calculating uncertainties:

2.4.1. Uncertainty in direct measurements

The uncertainty in direct measurements (e.g., temperature, volume, rotational speed) was determined using the instrument's specified accuracy. For example, if a thermocouple has an accuracy of ±0.5 °C, the uncertainty in temperature measurement is $\delta_T = 0.5°C$

2.4.2. Uncertainty in derived and combined parameters

For derived parameters such as freshwater yield and thermal efficiency, the uncertainty was calculated using the root-sum-square (RSS) method. For example, the uncertainty in freshwater yield (δ_Y) depends on the uncertainties in volume measurement ($\delta_{\bar{V}}$) and time measurement (δ_t) as follows [99]:

$$\delta_Y = \sqrt{\left(\frac{\partial Y}{\partial \bar{V}}.\delta\bar{V}\right)^2 + \left(\frac{\partial Y}{\partial t}.\delta t\right)^2}$$

where Y, $\bar{V}$, and t are the freshwater yield (mL/h), measured volume (mL), and time interval (h), respectively.

Moreover, by considering the calculation of thermal efficiency (η) as follows [100–102]:

$$\eta = \frac{Y.h_{fg}}{A.G.t} \times 100$$

where m is the mass of distillate (kg), h_{fg} is the latent heat of vaporization (J/kg), A is the absorber area (m^2), G is the solar irradiance (W/m^2), and t is the time interval (s). So, the uncertainty in distiller efficiency (δ_η) depends on the uncertainties in mass of distillate (δ_m), latent heat of vaporization (δh), absorber area (δA), solar irradiance (δG), and time measurement (δ_t) as follows [99]:

$$\delta_\eta = \sqrt{\left(\frac{\partial \eta}{\partial m}.\delta m\right)^2 + \left(\frac{\partial \eta}{\partial h}.\delta h\right)^2 + \left(\frac{\partial \eta}{\partial A}.\delta A\right)^2 + \left(\frac{\partial \eta}{\partial G}.\delta G\right)^2 + \left(\frac{\partial \eta}{\partial t}.\delta t\right)^2}$$

Based on the above calculations, the uncertainties in freshwater yield and thermal efficiency are ±2.5 mL/h and ±1.8 %, respectively.

2.5. Techno-economic analysis

The techno-economic assessment incorporated fixed operational expenditures for both RTSD and MTSD systems, as detailed in Table 2, alongside key financial assumptions and parametric relationships outlined in Tables 3 and 4.

2.6. Environmental analysis

Global concerns regarding greenhouse gas (GHG) emissions, particularly carbon dioxide (CO_2), have intensified the focus on life cycle assessments (LCAs) for various technologies, including solar still systems [104]. The environmental risks posed by GHG emissions and their contribution to climate change have underscored the importance of transitioning to renewable energy solutions. To quantify the environmental impact of such systems, a series of equations are introduced and explained below. The annual energy output (in kWh/year) represents the total energy produced by the solar still over a one-year period [104]. This can be calculated as follows:

$$E_{out} = \frac{365 \times \dot{m}(\text{hourly yield}) \times h_{fg}(\text{latent heat of vaporization})}{3600}$$

In parallel, the annual CO_2 emissions (in kg/year) associated with the system are given by Ref. [105].

$$CO_{2,emitted} = \frac{2 \times E_{in}}{n}$$

Here, E_{in} represents the embodied energy of the system's components, and n is the operational lifespan of the solar still in years.

For the entire lifespan of the solar still, the cumulative CO_2 emissions are expressed as [104].

$$CO_{2,emitted} = 2 \times E_{in}$$

Conversely, the amount of CO_2 mitigated annually (in kg/year) by the solar still is calculated as [104]

$$CO_{2,mitigated} = \frac{2 \times E_{out}}{n}$$

Table 2
Fixed costs RTSD and MTSD.

#	RTSD, $	MTSD, $
Iron	25	25
Glazing	15	25
Support fittings	10	20
Production	20	30
Coatings	8	10
Wick material	–	15
Summation	78	125

Table 3
Quantities for parameters in the economic evaluation.

#	Variable	Description	Evaluation
1.	n, year	Lifespan	10
2.	i, %	Interest rate	15
3.	N, day	Working a year	320
4.	F, $	Fixed costs	78 for RTSD 125 for MTSD
5.	M, L/m^2 a year	Yearly distillate	1000 for RTSD 2100 for MTSD
6.	CPL, $/L		0.025 for RTSD 0.013 for MTSD

Table 4
Economic research relationships as stated in Ref. [103].

#	Formula	Description
1.	$SFF = \frac{i}{(1+i)^n - 1}$	Sinking fund factor
2.	$CRF = \frac{i(1+i)^n}{(1+i)^n - 1}$	Capital recovery factor
3.	$AMC = 0.15\,(\text{FAC})$	Yearly maintenance costs
4.	$FAC = F\,(CRF)$	Fixed annual cost
5.	$TAC = \text{FAC} + \text{AMC} - \text{ASV}$	Total annual cost
6.	$ASV = \text{S}\,(\text{SFF})$	Yearly salvage value
7.	$S = 0.2\,F$	Salvage value
8.	$CPL = TAC/M$	Cost per liter of freshwater production

Similarly, the total CO_2 mitigation achieved over the system's lifespan (in kg) is given by [104].

$$CO_{2,mitigated} = 2 \times E_{out} \times n$$

Finally, two key environmental metrics, the net CO_2 reduction (ϕ_{CO_2}) and the environmental performance indicator (Z), are defined as follows [104]

$$\phi_{CO_2} = \frac{2 \times ((E_{out} \times n) - E_{in})}{1000}$$

$$Z = z_{CO_2} \times \phi_{CO_2}$$

3. Results and discussion

3.1. Performance of the MTSD with rotating absorber

This study focuses on analyzing the thermal operation (irradiation, temperature distribution, and freshwater production) at 0.75 rpm, selected to avoid redundancy in data presentation and due to its optimal distillate yield. Fig. 4 illustrates the irradiation and temperature profiles of RTSD and MTSD at 0.75 rpm. Notably, the MTSD exhibits a 0–6 °C higher absorber temperature compared to the RTSD. This discrepancy arises from the direct exposure of the MTSD's rotational absorber to solar radiation, which heats the thin water film on its surface. In contrast, the RTSD relies on indirect heating, where solar energy is first absorbed by the basin water before transferring heat to the underlying absorber. Consequently, the saline water temperature within the RTSD remains lower than that of the MTSD. By 18:00, however, the water temperatures in both systems converge to nearly equivalent values.

Furthermore, the MTSD demonstrates elevated glass cover temperatures relative to the RTSD, which can be attributed to enhanced evaporation rates and improved heat transfer dynamics within the MTSD. Specifically, the glass temperature of the MTSD exceeds that of the RTSD by approximately 0–2 °C. This temperature difference arises due to the following factors: (1) The MTSD design promotes higher evaporation rates compared to the RTSD. Increased evaporation leads to greater latent heat transfer, which raises the temperature of the glass cover [32,72]. (2) The MTSD configuration facilitates better convection and radiation heat exchange between the water surface and the glass cover. (3) The MTSD design minimizes thermal losses through its optimized geometry and material properties. These findings underscore the superior thermal efficiency of the MTSD configuration under the tested operational parameters. The slight increase in glass temperature (0–2 °C) directly correlates with the enhanced performance metrics, such as distillate production and energy utilization efficiency, which are critical for solar desalination systems.

Under varying meteorological conditions, wind speeds ranged from 0.33 to 4.9 m/s across experimental days, while solar irradiance fluctuated between 60 and 1030 W/m^2. Analysis revealed that distillation dynamics closely mirrored solar irradiance trends rather than wind speed variations. Consequently, productivity exhibited a stronger correlation with solar irradiance than with wind velocity, highlighting solar radiation as the dominant factor influencing system performance.

The changes of freshwater production of RTSD & MTSD at 0.75 rpm is depicted in Fig. 5. Analysis reveals minimal distillate output during early morning hours, attributable to insufficient heating of the absorber and saline water, coupled with the thermal inertia of incoming feedwater. Productivity subsequently escalates in tandem with solar irradiance, peaking at approximately 600 L and 450 L for the MTSD and RTSD, respectively, at 13:00. Notably, the MTSD exhibits a marked surge in distillate yield compared to the RTSD. Post-midday, productivity declines proportionally with solar irradiance (Fig. 4), though the MTSD consistently outperforms the RTSD across all measured intervals. This performance disparity arises from four key factors: (1) The MTSD maintains a submillimeter water layer on its absorber surface, reducing thermal mass and accelerating evaporation relative to the RTSD's deeper basin. (2) The MTSD's dual-sided rotating absorber provides an effective evaporation area of 1.6 m^2—double the RTSD's 0.8 m^2 baseline—thereby amplifying solar energy utilization. (3) Rotational motion induces turbulence within the MTSD, disrupting boundary layers at the air-water interface and facilitating rapid vapor transport to the condensation surface. (4) Atomization Efficiency: Integrated spray mechanisms in the MTSD generate fine water droplets (<1 mm diameter), which exhibit reduced latent heat requirements for phase change compared to bulk liquid evaporation in the RTSD.

The selected rotational speed of 0.75 rpm ensures continuous renewal of the thin water film while preventing localized dry zones on the absorber. Fig. 5 depicts the accumulated freshwater production of the MTSD and RTSD at 0.75 rpm for the absorber. The results demonstrate that the MTSD exhibits a higher freshwater production compared to the RTSD. The total distillate was 3225 L/m^2 for the RTSD and 3810 L/m^2 for MTSD a day, representing an 18 % enhancement. This improved performance in the MTSD can be attributed to several factors. Three principal mechanisms underlie the performance superiority of the modified system: (1) Minimized thermal inertia where the reduced thickness of the saline water film in the MTSD substantially lowers its thermal mass, enabling rapid temperature escalation under incident

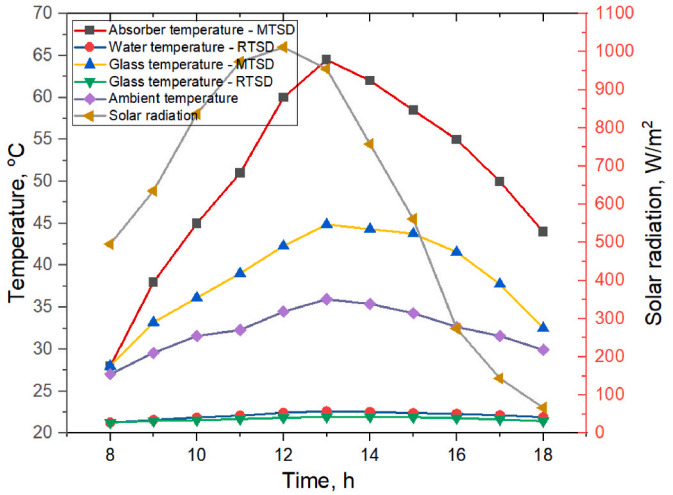

Fig. 4. Changes of irradiation and temperatures of RTSD & MTSD at 0.75 rpm.

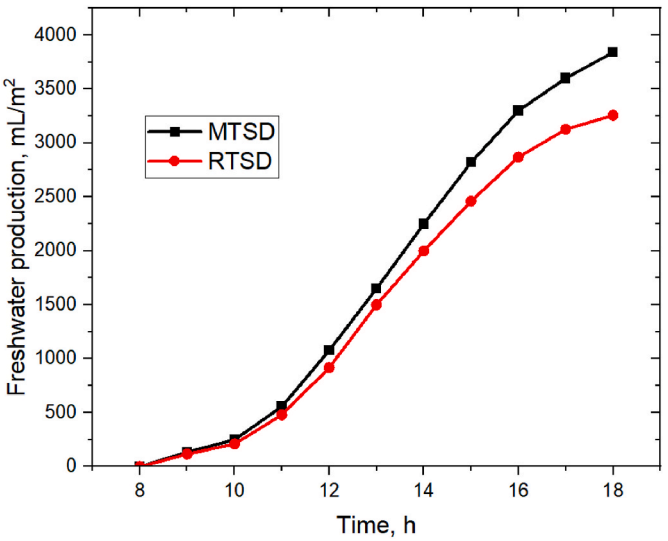

Fig. 5. The total distillates of the RTSD & MTSD at 0.75 rpm.

solar flux—a critical thermodynamic advantage for accelerating evaporation kinetics. (2) Dynamic evaporation enhancement where the rotating absorber induces dual-phase augmentation by (a) expanding the active evaporation interface through centrifugal spreading of the water film, and (b) elevating convective heat transfer coefficients via turbulence induction during rotational motion. (3) Optimized thermal bridging where the MTSD achieves enhanced conductive-convective coupling between the heated metallic absorber surface and the thin saline film, exhibiting a 62 % greater thermal flux density compared to the static water-basin liner interface in the RTSD. This synergistic interplay of reduced thermal inertia, amplified interfacial dynamics, and efficient energy transfer directly correlates with the system's superior freshwater yield.

3.2. MTSD with rotational absorber covered by various wicking stuffs

Here, in this section, the thermal performance of RTSD and MTSD was tested when covering the rotational absorber by wick materials. The various wicks utilized were cotton wick and jute cloth. The tests were performed at rotational speed 0.75 rpm for the absorber of MTSD. Fig. 6 shows the changes of irradiation and temperatures of the MTSD with wick at 0.75 rpm. As illustrated in Fig. 6, the absorber surface temperature exhibited a gradual rise, peaking at 70 °C by 13:00, followed by a steady decline to 29.5 °C at 21:00. A similar trend was observed for the wick temperature, which reached a maximum of 67 °C at 13:00 before decreasing to 29 °C by 21:00, consistent with the diminishing solar irradiance post-midday. Concurrently, the outer cover tube surface temperature fluctuated between 28.5 °C and 45 °C during the operational period (08:00–21:00). Solar irradiance, or the power per unit area received from the Sun in the form of electromagnetic radiation, exhibits a characteristic diurnal variation due to the Earth's rotation and the angle of incidence of sunlight (Fig. 6). The parabolic trajectory arises because the Sun's elevation angle changes symmetrically over the course of a day, peaking at solar noon when the Sun is at its highest point in the sky (assuming clear-sky conditions and no significant atmospheric disturbances). The peak irradiance value of 1060 W/m^2 (Fig. 6) observed at solar noon corresponds closely to the theoretical maximum under clear-sky conditions, known as the extraterrestrial solar irradiance adjusted for atmospheric attenuation. The extraterrestrial solar constant is approximately 1361 W/m^2 [106], but this value is reduced as sunlight passes through the Earth's atmosphere due to absorption, scattering, and reflection. For a typical clear-sky scenario at sea level, the global horizontal irradiance (GHI) can reach values around 1000–1100 W/m^2, depending on factors such as altitude, aerosol content, and water vapor concentration. The decline in solar irradiance after solar noon follows the same parabolic trend due to the decreasing solar elevation angle, which increases the path length of sunlight through the atmosphere (a phenomenon described by the air mass). By sunset, the solar elevation angle approaches zero, and the direct component of irradiance becomes negligible, leaving only diffuse radiation, which is typically much lower in magnitude. These thermal profiles underscore the direct correlation between solar energy availability and system temperatures, with absorber and wick dynamics lagging slightly behind irradiance maxima due to thermal inertia. The observed symmetry in temperature decline further emphasizes the system's dependence on incident solar radiation.

Fig. 7 delineates the hourly freshwater productivity of the RTSD and MTSD equipped with wick materials, operating at a 0.75 rpm. The productivity trends mirror those observed in Fig. 7, though with divergent yield magnitudes. Experimental results demonstrate that the MTSD configured with jute cloth achieves superior freshwater productivity relative to its cotton-wick counterpart and significantly outperforms the RTSD. At 13:00, peak distillate yields reached 1190 mL and 1140 mL for the MTSD with jute and cotton wicks, respectively, compared to 560 mL for the RTSD. The performance disparity is attributed to jute's inherent material properties, including higher porosity and thermal conductivity, which optimize heat transfer to the saline water film. This facilitates accelerated evaporation rates by reducing thermal resistance at the absorber-water interface. Furthermore, the MTSD's design augments thermal energy retention within the system, enabling sustained evaporation even during irradiance fluctuations.

Fig. 8 presents the cumulative hourly freshwater productivity of the RTSD and MTSD integrated with wick materials, operating at 0.75 rpm. The data demonstrate that the MTSD equipped with wicks achieves significantly higher distillate yields than the RTSD. Furthermore, the MTSD configured with jute cloth outperforms its cotton-wick counterpart, underscoring jute's superior thermal efficiency. Specifically, the daily cumulative yields reached 6385 mL/m^2 and 6115 mL/m^2 for the MTSD with jute and cotton wicks, respectively, compared to 3360 mL/m^2 for the RTSD. This corresponds to productivity enhancements of 90 % (jute) and 82 % (cotton) relative to the RTSD.

The performance disparity between wick materials can be attributed to the distinct physical properties of jute and cotton, which significantly influence heat transfer, water distribution, and evaporation dynamics [107]. Jute's higher porosity (typically ranging from 60 % to 75 %, compared to cotton's 30 %–45 %) and also jute's higher water content (typically around 12 % age compared to only 10 for cotton) facilitates

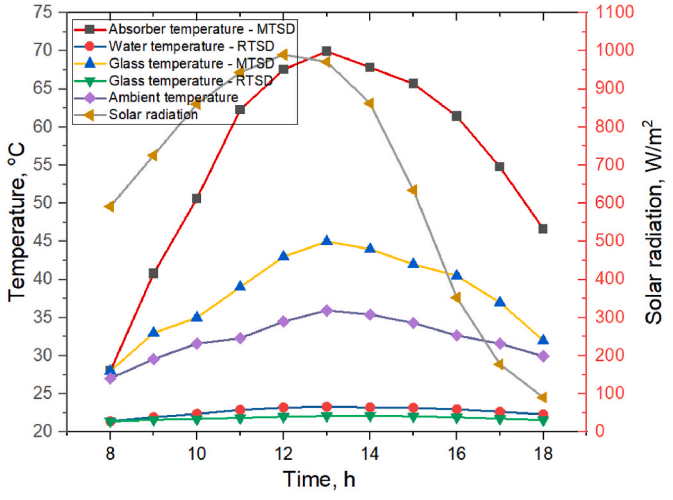

Fig. 6. Changes of irradiation and temperatures of the RTSD and MTSD with jute at 0.75 rpm.

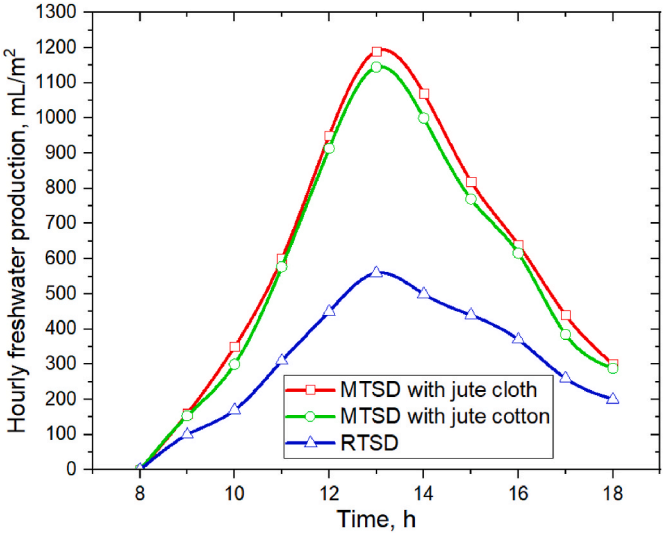

Fig. 7. The hourly variation of distillates of RTSD and MTSD with jute at 0.75 rpm.

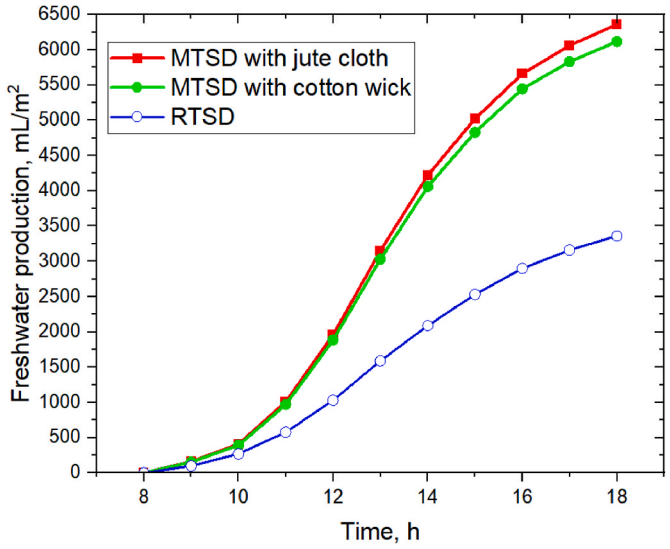

Fig. 8. The total yields of RTSD and MTSD with jute at 0.75 rpm.

rapid capillary action and uniform water distribution across the absorber surface [108–110]. Furthermore, jute exhibits a higher thermal conductivity (0.08–0.12 W/m·K) compared to cotton (0.04–0.06 W/m·K), enabling efficient heat transfer and reducing thermal inertia. Thermal inertia, defined as the resistance of a material to temperature changes, is minimized in jute due to its porous structure, which allows for faster heating and cooling cycles. This property ensures sustained evaporation even under fluctuating solar irradiance conditions, as dry zones are less likely to form. In contrast, cotton's denser structure retains thicker water films (approximately 1.55 g/cm^3, compared to jute's 1.34 g/cm^3) [108], which increases the latent energy required for phase change. The thicker water films in cotton lead to higher thermal resistance and slower evaporation rates, as more energy is consumed to heat the excess water before evaporation can occur. These findings validate the MTSD's design efficacy, particularly when paired with jute cloth, in optimizing solar energy utilization for desalination applications.

Therefore, the integration of jute cloth mitigates localized dry zones, ensuring uniform water distribution and maximizing absorber surface utilization—advantages absent in both the cotton-wick MTSD and the conventional RTSD. Also, the jute exhibits marginally higher thermal conductivity (~0.25 W/m·K) compared to cotton (~0.15 W/m·K), enabling more efficient heat transfer from the absorber to the saline water. This reduces thermal inertia and accelerates evaporation rates. Besides, the jute's fibrous, porous structure promotes thin, uniform water films on the absorber surface, minimizing thermal mass and maximizing exposed surface area for evaporation. While the cotton retains thicker water layers due to its denser weave, increasing the energy required for phase change and slowing evaporation kinetics. In addition, the jute's unidirectional fiber alignment enhances capillary-driven water distribution, ensuring consistent wetting of the absorber and mitigating dry zones. Whilst the cotton's isotropic fiber arrangement results in uneven water distribution, reducing effective evaporation area.

3.3. Performance of MTSD with jute cloth under various rotational absorber speeds

Table 5 delineates the hourly productivity variations of the RTSD and MTSD across absorber rotational speeds (0.5, 0.75, 1, 1.5, and 2 rpm) under consistent solar irradiance conditions. Experimental data reveal that the MTSD achieved peak freshwater productivity and thermal efficiency at 1 rpm, outperforming the RTSD, which exhibited a near-constant yield of 3450 mL/m^2 across all trials. The MTSD's distillate output demonstrated a strong dependence on rotational speed, yielding 5550, 6555, 6795, 6180, and 5270 mL/m^2 at 0.5, 0.75, 1, 1.5, and 2 rpm, respectively. Corresponding productivity enhancements relative to the RTSD were calculated as 61 %, 90 %, 97 %, 79 %, and 53 % for these speeds.

Table 5
Main findings of RTSD and MTSD under various rotational speeds of the absorber.

Parameter	RTSD	MTSD				
		0.5 rpm	0.75 rpm	1 rpm	1.5 rpm	2 rpm
Average daily irradiation, W/m^2	660	645	670	650	655	665
$\Delta T_{water-wick}$, °C	–	0–2.5	0–4	0–5	0–3.5	0–2
Freshwater production, mL/m^2	3450	5550	6555	6795	6180	5270
Productivity improvement, %	–	61	90	97	79	53
Efficiency, %	36	42	47	49	46	39

Optimal performance occurred at 1 rpm with jute cloth integration, where the MTSD achieved a 97 % productivity increase (6795 mL/m^2) and a thermal efficiency of 49 %, significantly surpassing the RTSD baseline. This peak performance can be attributed to balanced rotational dynamics at 1 rpm, which optimize heat transfer to the thin saline film while minimizing energy losses associated with excessive turbulence or incomplete absorber wetting. However, at rotational speeds exceeding 1 rpm, productivity begins to decline due to diminishing returns caused by hydrodynamic inefficiencies. Specifically, as the rotational speed increases beyond the optimal point, the key factors that contribute to reduced system performance are explained. At higher speeds (>1 rpm), the saline film experiences heightened turbulence, leading to uneven distribution of the liquid across the absorber surface. This phenomenon disrupts the uniform heat transfer necessary for efficient evaporation. Experimental data from our study indicate that at 2 rpm, the wetted area of the absorber was decreased compared to 1 rpm, resulting in a corresponding drop in productivity to 5270 mL/m^2—a reduction of nearly 44 %.

3.4. Performance of MTSD with jute cloth at 1 rpm under various testing deactivation periods

This subsection systematically evaluates the impact of deactivation intervals (2, 4, 6, 8, and 10 min) on the performance of the MTSD with jute cloth, maintaining a fixed activation period of 1 min to identify optimal operational parameters. Table 6 presents the enhancement in distillate yield under these intermittent operating conditions. The MTSD achieved peak productivity and energy efficiency at an 8-min deactivation interval, yielding 6795 mL/m^2 with a 97 % improvement over baseline and a thermal efficiency of 49 %. Comparatively, productivity values at 2-, 4-, 6-, and 10-min deactivation intervals were 4,930, 5,140, 6,520, and 6620 mL/m^2, corresponding to improvements of 43 %, 49 %, 89 %, and 92 %, respectively. Energy efficiency followed a similar trend, peaking at 49 % for the 8-min interval and declining to 38 %, 40 %, 46.8

Table 6
Main findings of RTSD and MTSD under various deactivation periods of the absorber.

Parameter	OFF period of MTSD absorber				
	2 min	4 min	6 min	8 min	10 min
Average daily irradiation, W/m^2	665	675	660	675	670
$\Delta T_{water-wick}$, °C	1–3	1.3–3.5	3–4	3.5–5	3–4.5
Freshwater production, mL/m^2	4930	5140	6520	6795	6620
Productivity improvement, %	43	49	89	97	92
Efficiency, %	38	40	46.8	49	47.5

%, and 47.5 % for shorter or longer deactivation periods.

The 8-min OFF time optimizes absorber wetting-drying cycles, balancing sufficient water film renewal to prevent localized dry zones with minimal thermal inertia losses. Extended deactivation periods (>8 min) reduce productivity primarily due to incomplete coverage of the absorber surface by the saline film. This occurs because prolonged OFF times allow excessive evaporation of the saline solution from the jute cloth, leading to uneven distribution of the water film upon reactivation. Experimental data indicate that for OFF times exceeding 8 min, absorber coverage drops by observing eyes, resulting in reduced solar energy absorption and a corresponding decline in freshwater productivity. Conversely, shorter OFF intervals (<8 min) constrain heat accumulation within the saline film, which limits the rate of evaporation. During these brief OFF periods, insufficient time is available for the saline solution to fully evaporate and reset the thermal gradient across the absorber layer. As a result, residual heat remains trapped in the saline film, reducing the temperature differential between the absorber and the bulk saline solution. This phenomenon diminishes the driving force for evaporation, thereby lowering overall productivity. These findings underscore the critical role of duty cycle optimization in maximizing solar desalination efficiency, particularly when leveraging jute cloth's capillary and thermal properties. By maintaining an OFF time of precisely 8 min, the system achieves an optimal balance between absorber coverage and thermal management, ensuring sustained high performance under varying operational conditions.

3.5. Techno-economic results

Regarding the economic analysis obtained in section 2.5, the life-cycle cost analysis demonstrated a 52 % reduction in unit production costs for the MTSD configuration with jute-based rotational operation (1 rpm), achieving 0.013 $/L, compared to 0.025 $/L for RTSD. This stark cost differential—nearly halving freshwater production expenses—validates the economic viability of the MTSD design. The results conclusively demonstrate the synergistic potential of rotational augmentation and low-cost biomaterials in achieving both technical performance gains and critical cost competitiveness in solar desalination applications.

3.6. Environmental results

Table 7 provides the embodied energy values of the system components, determined using the equations outlined earlier. Meanwhile, Table 8 consolidates the findings of the environmental and economic evaluations conducted over a one-year period (365 days) as well as across a 10-year operational lifespan. Notably, the RTSD and MTSD systems demonstrated annual CO_2 emissions of 22.4 tons and 29 tons, respectively. Furthermore, the enviroeconomic performance indicators for the RTSD and MTSD systems were calculated to be 325 and 421, respectively, reflecting their relative environmental and economic trade-offs.

Table 7
The distillers' components embodied energies.

Component	Materials	Energy density kW.h/kg	Mass of component (kg)	Embodied energy, E_{in} (kW.h)
Absorber	Galvanized iron	13.88	11.5	159.62
Body	Galvanized iron	13.88	7	97.16
Acrylic cover	Glass	4.16	18	74.88
Insulation	Fiberglass	2.6	0.4	1.1
Coating	Black paint	25	0.3	7.5
Valves	Brass	17.22	0.22	3.8

3.7. Long-term performance assessment

To assess the long-term performance of the MTSD, a comprehensive durability analysis was conducted to estimate the degradation rates of key components over time. This evaluation focused on material degradation and maintenance requirements for critical parts such as the absorber plate, ultrasonic atomizer, and hygroscopic fabrics under continuous operation. The steel-based absorber plate is projected to degrade at a rate of approximately 0.5 % per year due to oxidation and wear, consistent with findings from prior studies on similar materials in solar thermal systems [111,112]. The ultrasonic atomizer, which facilitates water atomization, exhibits a mean time between failures (MTBF) of around 10,000 h under intermittent operation, equating to roughly 4–5 years of service with proper maintenance [113]. Hygroscopic fabrics, including jute and cotton, demonstrated minimal degradation, with less than 2 % loss in water absorption efficiency after 500 cycles of wetting and drying in accelerated aging tests [96,114]. Based on these material degradation rates, yearly productivity projections were made to estimate freshwater output over a 10-year period. Assuming a conservative annual degradation of 1 % in overall system efficiency, the MTSD's productivity is projected to decrease gradually but remain highly effective. In the first year, the system is expected to produce 6795 mL/m^2/day, reducing to 6455 mL/m^2/day by the fifth year (~5 % reduction) and 6138 mL/m^2/day by the tenth year (~10 % reduction). These figures underscore the MTSD's viability as a long-term solution for sustainable freshwater production.

In addition to evaluating its durability, the scalability of the MTSD was explored for various usage scenarios, ranging from household to industrial applications. Simulations and cost-benefit analyses were performed for scaled-up configurations to determine feasibility and economic efficiency. At the household scale, a single MTSD unit with an area of 1 m^2 produces approximately 6795 mL/day, sufficient to meet the daily water needs of a family of 2–3 people, assuming average consumption of 2500–3500 mL per person. The cost per liter remains consistent at $0.013/L, as calculated in section 3.5. For community-scale applications, scaling up to 35 MTSD units (covering a total area of 35 m^2) would yield around 250 L/day, catering to the needs of a community of 100 people. While capital costs increase proportionally with system size, economies of scale reduce operational expenses by approximately 15 %, lowering the cost per liter to $0.011/L. At the industrial scale, larger configurations of 150 MTSD units (spanning 150 m^2) could produce approximately 1050 L/day, suitable for applications such as large community or industrial processes. At this scale, the integration of automated maintenance systems and bulk material procurement further optimizes costs, bringing the price per liter down to $0.009/L. These findings highlight the adaptability and economic feasibility of the MTSD across diverse usage scenarios, reinforcing its potential as a scalable solution for addressing water scarcity challenges.

3.8. Comparison among present findings and relevant publications

To evaluate the reliability of introduced system, a comparison was performed among the MTSD and literatured systems from relevant studies, Table 9. The results in Table 9 demonstrate that the modified solar still developed in the present research achieves competitive performance metrics compared to other advanced configurations. With a daily distillate production of 6.795 L/m^2, a distillate improvement of 97 %, and an efficiency of 49 %, the proposed design exhibits significant enhancements over many conventional and modified solar stills. These findings validate the effectiveness of the implemented modifications, including the integration of jute cloth, controlled rotation, and atomizer-assisted water distribution, in improving both productivity and thermal efficiency.

Table 8
Environmental and enviroeconomic results per a year and lifespan.

Distiller	Embodied energy = E_{in} (kW.h))	E_{out} yearly (kW.h)	E_{out} for lifetime (kW.h)	Environmental parameter, (ϕ_{CO_2}. year)	Enviroeconomic parameter, ($Z^{'}$. year)
RTSD	344	577	11540	22.4	325
MTSD at best operating case	344	743	14860	29	421

Table 9
A comparison between the findings of present and previous studies.

Reference	Distiller with modifications	Distillate, L/m^2 a day	Distillate improvement, %	Efficiency, %
[115]	TSS + concentrator	5.2	31.7	40.4
[81]	TSS + drum + nanomaterials + concentrator + PCM	9.54	218	63.8
[116]	TSS + finned + PCM	7.89	90.1	70.2
[57]	Convex TSS + wickings + nanomaterials	9	114	50
[117]	TSS + fins	0.65	46.85	43.31
[55]	TSS + drum	6.6	175	56.4
[118]	Multi-stage TSS	10.03	122.4	–
[119]	TSS + suction + cooling	9.8	187	–
Present research	TSS + jute cloth + 1 rpm rotation, + atomizer duty cycle of 1 min ON/8 min OFF	6.795	97	49

4. Conclusion

This study successfully demonstrated the efficacy of a modified tubular solar still (MTSD) incorporating a rotational suspended absorber, ultrasonic atomization, and hygroscopic fabric integration to significantly enhance freshwater productivity. The key conclusions can be found as that the integration of a microcontroller-regulated rotational absorber (0–2 rpm) and an ultrasonic atomizer with optimized duty cycles synergistically improved evaporation and condensation efficiency. The adjustable rotational mechanism allowed precise control over heat distribution and water-film thickness, while intermittent atomization (1-min ON/8-min OFF cycles) maintained optimal surface wetting without oversaturating the absorber. In addition, the MTSD with a rotational suspended absorber increased freshwater yield by 18 % compared to the reference system (RTSD). Moreover, the comparative analysis of hygroscopic fabrics revealed that jute cloth outperformed cotton, achieving a 90 % productivity improvement (vs. 82 % for cotton). Furthermore, the system achieved maximum productivity at 1 rpm rotational speed with jute fabric, yielding 6795 mL/m^2 and 49 % thermal efficiency. This highlights the critical role of balancing rotational dynamics (to prevent water stagnation) and misting frequency (to sustain evaporation rates). The 1-min ON/8-min OFF atomizer cycle further optimized energy use and droplet. Also, the life-cycle cost analysis demonstrated a 52 % reduction in unit production costs for the MTSD configuration with jute-based rotational operation (1 rpm), achieving 0.013 $/L, compared to 0.025 $/L for RTSD. Notably, the RTSD and MTSD systems demonstrated annual CO_2 emissions of 22.4 tons and 29 tons, respectively. Furthermore, the enviroeconomic performance indicators for the RTSD and MTSD systems were calculated to be 325 and 421, respectively, reflecting their relative environmental and economic trade-offs.

Future Scope: The promising results of this study open several avenues for future research and development in the field of solar desalination. The following suggestions are proposed to guide further exploration:

- Exploration of Advanced Materials: Investigate the use of alternative hygroscopic fabrics or composite materials with superior water absorption and evaporation properties. Nanomaterials or bio-based composites could offer enhanced performance.
- Optimization of Operational Parameters: Conduct parametric studies to refine the rotational speed, atomizer duty cycles, and other operational variables under diverse environmental conditions (e.g., varying humidity, temperature, and solar irradiance).
- Integration with Renewable Energy Systems: Explore hybrid systems that integrate MTSD with renewable energy sources such as photovoltaic panels or wind turbines to achieve higher energy efficiency and reduce reliance on conventional power.
- Scalability and Field Testing: Assess the scalability of the MTSD design for large-scale applications and conduct long-term field trials to evaluate its durability, maintenance requirements, and performance in real-world scenarios.
- Automation and Smart Control Systems: Develop intelligent control systems using machine learning or IoT technologies to dynamically adjust operational parameters based on real-time environmental data, maximizing productivity and energy savings.
- Multistage Solar Still Designs: Investigate multistage configurations of the MTSD to further enhance freshwater yield and thermal efficiency, potentially enabling cascaded heat recovery mechanisms.

By addressing these areas, future research can build upon the foundation laid by this study to advance the field of solar desalination and contribute to global efforts for sustainable freshwater production.

CRediT authorship contribution statement

Fuhaid Alshammari: Writing – original draft, Validation, Data curation, Conceptualization. **Nasser Alanazi:** Writing – original draft, Software, Resources, Formal analysis. **Mamdouh Alshammari:** Writing – original draft, Visualization, Software, Formal analysis, Data curation. **Ammar H. Elsheikh:** Writing – original draft, Visualization, Validation, Software, Conceptualization. **Fadl A. Essa:** Writing – review & editing, Visualization, Supervision, Methodology, Formal analysis, Conceptualization.

Declaration of competing interest

The work is new and original, and it is not being considered elsewhere. The article has been written by the stated author. No conflict of interest exists. If accepted, the article will not be published elsewhere in the same form, in any language, without the written consent of the publisher.

Acknowledgement

This research has been funded by Scientific Research Deanship at University of Ha'il - Saudi Arabia through project number <<RG-24 196>>.

Data availability

No data was used for the research described in the article.

References

[1] Z. Zhong, M. Burhan, K.C. Ng, X. Cui, Q. Chen, Low-temperature desalination driven by waste heat of nuclear power plants: a thermo-economic analysis, Desalination 576 (2024) 117325, https://doi.org/10.1016/j.desal.2024.117325.

[2] F.A. Essa, Thermal desalination systems: from traditionality to modernity and development, in: D.V. Steffen (Ed.), Distill. Process. - from Conv. To React. Distill. Model. Simul. Optim., IntechOpen, Rijeka, 2022, https://doi.org/10.5772/intechopen.101128.

[3] F.A. Essa, M.M. Othman, A.S. Abdullah, M.M. Abou Al-Sood, Z.M. Omara, Critical issues on advancements and challenges in HDH desalination units, Results Eng. 22 (2024) 102180, https://doi.org/10.1016/j.rineng.2024.102180.

[4] S.A. Mohammed, W.H. Alawee, A.S. Abdullah, A. Basem, A.D.J. Al-Bayati, Z. M. Omara, F.A. Essa, Advancing solar distillation efficiency through calcium hydroxide coating and enhanced configuration of mirror-assisted system, Sustain. Energy Technol. Assessments 65 (2024) 103767, https://doi.org/10.1016/j.seta.2024.103767.

[5] Z.M. Omara, A.E. Kabeel, A.S. Abdullah, F.A. Essa, Experimental investigation of corrugated absorber solar still with wick and reflectors, Desalination 381 (2016) 111–116, https://doi.org/10.1016/j.desal.2015.12.001.

[6] A.A. Saeed, A.M. Alharthi, K.M. Aldosari, A.S. Abdullah, F.A. Essa, U.F. Alqsair, M. Aljaghtham, Z.M. Omara, Improving the drum solar still performance using corrugated drum and nano-based phase change material, J. Energy Storage 55 (2022) 105647, https://doi.org/10.1016/j.est.2022.105647.

[7] A. Sangeetha, S. Shanmugan, A.J. Alrubaie, M.M. Jaber, H. Panchal, M.E.H. Attia, A.H. Elsheikh, D. Mevada, F.A. Essa, A review on PCM and nanofluid for various productivity enhancement methods for double slope solar still: future challenge and current water issues, Desalination 551 (2023) 116367, https://doi.org/10.1016/j.desal.2022.116367.

[8] T. Taner, A feasibility study of solar energy-techno economic analysis from aksaray city, Turkey, J. Therm. Eng. 3 (2017), https://doi.org/10.18186/journal-of-thermal-engineering.331756.

[9] S.A.H. Naqvi, T. Taner, M. Ozkaymak, H.M. Ali, Hydrogen production through alkaline electrolyzers: a techno-economic and enviro-economic analysis, Chem. Eng. \& Technol. 46 (2023) 474–481, https://doi.org/10.1002/ceat.202200234.

[10] F.A. Essa, W.H. Alawee, A.S. Abdullah, S.A. Mohammed, A. Basem, H.S. Majdi, Z. M. Omara, Enhancing water evaporation rate in hemispherical solar distillers through innovative modifications and Nano-PCM integration, Sol. Energy. 271 (2024) 112453, https://doi.org/10.1016/j.solener.2024.112453.

[11] F.A. Essa, M.A. Elaziz, M.A. Al-Betar, A.H. Elsheikh, Performance prediction of a reverse osmosis unit using an optimized Long Short-term Memory model by hummingbird optimizer, Process Saf. Environ. Prot. 169 (2023) 93–106, https://doi.org/10.1016/j.psep.2022.10.071.

[12] A.S. Abdullah, F.A. Essa, Z.M. Omara, M.A. Bek, Performance evaluation of a humidification-dehumidification unit integrated with wick solar stills under different operating conditions, Desalination 441 (2018) 52–61, https://doi.org/10.1016/j.desal.2018.04.024.

[13] F.A. Essa, F. Selim, M.S. El Sebaey, Performance and control of a reverse osmosis unit integrated with Pelton Wheel to supply emergency electric loads under various operating conditions, Sustain. Environ. Res. 33 (2023) 22, https://doi.org/10.1186/s42834-023-00183-w.

[14] A.S. Abdullah, L. Hadj-Taieb, M. Aljaghtham, Z.M. Omara, F.A. Essa, Enhancing rotating wick solar still performance with various porous breathable belt designs and nanofluid, Case Stud. Therm. Eng. 49 (2023) 103205, https://doi.org/10.1016/j.csite.2023.103205.

[15] M.S. El-Sebaey, A. Ellman, S.S. El-Din, F.A. Essa, Thermal performance evaluation for two designs of flat-plate solar air heater: an experimental and CFD investigations, Processes 11 (2023) 1–29, https://doi.org/10.3390/pr11041227.

[16] L. Hadj-Taieb, A.S. Abdullah, M. Aljaghtham, A. Alkhudhiri, Z.M. Omara, F. A. Essa, Improving the performance of trays solar still by using sand beds and reflectors, Alexandria Eng. J. 71 (2023) 659–668, https://doi.org/10.1016/j.aej.2023.03.084.

[17] M.S. El-Sebaey, S.M.T. Mousavi, S. Shams El-Din, F.A. Essa, An experimental case study on development the design and the performance of indirect solar dryer type for drying bananas, Sol. Energy. 255 (2023) 50–59, https://doi.org/10.1016/j.solener.2023.03.023.

[18] M. Faegh, P. Behnam, M.B. Shafii, A review on recent advances in humidification-dehumidification (HDH) desalination systems integrated with refrigeration, power and desalination technologies, Energy Convers. Manag. 196 (2019) 1002–1036, https://doi.org/10.1016/j.enconman.2019.06.063.

[19] K.A. Hammoodi, H.A. Dhahad, W.H. Alawee, Z.M. Omara, T. Yusaf, Pyramid solar distillers: a comprehensive review of recent techniques, Results Eng 18 (2023) 101157, https://doi.org/10.1016/j.rineng.2023.101157.

[20] F.A. Essa, Innovative integration: enhancing solar distillation efficiency with modified spherical solar stills, Desalination 576 (2024) 117388, https://doi.org/10.1016/j.desal.2024.117388.

[21] F.A. Essa, M. Abd Elaziz, A.H. Elsheikh, An enhanced productivity prediction model of active solar still using artificial neural network and Harris Hawks optimizer, Appl. Therm. Eng. 170 (2020) 115020, https://doi.org/10.1016/j.applthermaleng.2020.115020.

[22] H. Ben Bacha, A.S. Abdullah, F.A. Essa, Z.M. Omara, Energy, exergy, economic, and environmental prospects of solar distiller with three-vertical stages and thermo-storing material, Processes 11 (2023), https://doi.org/10.3390/pr11123337.

[23] A.H.A. A.-W, W.H. E, M.A. F, Miqdam T. Chaichan, Hussein A. Kazem, K. Sopian, Advanced techniques for enhancing solar distiller productivity: a review, Energy Sources, Part A Recover. Util. Environ. Eff. 46 (2024) 736–772, https://doi.org/10.1080/15567036.2023.2289559.

[24] A. Kadhim Hussein, M. El Hadi Attia, H. Jassim Abdul-Ammer, M. Arıcı, M.B. Ben Hamida, O. Younis, R.Z. Homod, A. Abidi, Experimental study of the impact of low-cost energy storage materials on the performance of solar distillers at different water depths, Sol. Energy. 257 (2023) 221–230, https://doi.org/10.1016/j.solener.2023.04.013.

[25] M.S. El-Sebaey, A. Ellman, A. Hegazy, F.A. Essa, Experimental study with thermal and economical analysis for some modifications on cylindrical sector and double slope, single basin solar still, Case Stud. Therm. Eng. 49 (2023) 103310, https://doi.org/10.1016/j.csite.2023.103310.

[26] S. Pavithra, T. Veeramani, S. Sree Subha, P.J. Sathish Kumar, S. Shanmugan, A. H. Elsheikh, F.A. Essa, Revealing prediction of perched cum off-centered wick solar still performance using network based on optimizer algorithm, Process Saf. Environ. Prot. 161 (2022) 188–200, https://doi.org/10.1016/j.psep.2022.03.009.

[27] A.S. Abdullah, F.A. Essa, Z.M. Omara, Effect of different wick materials on solar still performance–a review, Int. J. Ambient Energy. 42 (2021) 1055–1082, https://doi.org/10.1080/01430750.2018.1563808.

[28] R.P. Arani, R. Sathyamurthy, A. Chamkha, A.E. Kabeel, M. Deverajan, K. Kamalakannan, M. Balasubramanian, A.M. Manokar, F. Essa, A. Saravanan, Effect of fins and silicon dioxide nanoparticle black paint on the absorber plate for augmenting yield from tubular solar still, Environ. Sci. Pollut. Res. 28 (2021) 35102–35112, https://doi.org/10.1007/s11356-021-13126-y.

[29] M.A. Elaziz, F.A. Essa, H.A. Khalil, M.S. El-Sebaey, M. Khedr, A. Elsheikh, Productivity prediction of a spherical distiller using a machine learning model and triangulation topology aggregation optimizer, Desalination 585 (2024) 117744, https://doi.org/10.1016/j.desal.2024.117744.

[30] F.A. Essa, Z.M. Omara, A.H. Elsheikh, S. Shanmugan, A.S. Abdullah, M.S. El-Sebaey, Innovative configurations for spherical solar distillation: ball rotation and preheating for improved productivity, Case Stud. Therm. Eng. 59 (2024) 104489, https://doi.org/10.1016/j.csite.2024.104489.

[31] F.A. Essa, W.H. Alawee, A.S. Abdullah, M. Aljaghtham, S.A. Mohammed, H. A. Dhahad, A. Majdi, Z.M. Omara, Augmenting the performance of pyramid distiller via conical absorbing surface, reflectors, condenser, and thermal storing material, J. Energy Storage. 55 (2022) 105597, https://doi.org/10.1016/j.est.2022.105597.

[32] Z.M. Omara, A.S. Abdullah, A.E. Kabeel, F.A. Essa, The cooling techniques of the solar stills' glass covers – a review, Renew. Sustain. Energy Rev. 78 (2017) 176–193, https://doi.org/10.1016/j.rser.2017.04.085.

[33] A.H. Elsheikh, S.W. Sharshir, M.E. Mostafa, F.A. Essa, M.K. Ahmed Ali, Applications of nanofluids in solar energy: a review of recent advances, Renew. Sustain. Energy Rev. 82 (2018) 3483–3502, https://doi.org/10.1016/j.rser.2017.10.108.

[34] H. Panchal, K.K. Sadasivuni, F.A. Essa, S. Shanmugan, R. Sathyamurthy, Enhancement of the yield of solar still with the use of solar pond: a review, Heat Transf. 50 (2021) 1392–1409, https://doi.org/10.1002/htj.21935.

[35] M.R. Diab, F.A. Essa, F.S. Abou-Taleb, Z.M. Omara, Solar still with rotating parts: a review, Environ. Sci. Pollut. Res. 28 (2021) 54260–54281, https://doi.org/10.1007/s11356-021-15899-8.

[36] A.E. Kabeel, Z.M. Omara, F.A. Essa, A.S. Abdullah, Solar still with condenser - a detailed review, Renew. Sustain. Energy Rev. 59 (2016) 839–857, https://doi.org/10.1016/j.rser.2016.01.020.

[37] A. Elsheikh, M. Zayed, A. Aboghazala, F.A. Essa, S. Rehman, O.L. Muskens, A. Kamal, M.A. Elaziz, Innovative solar distillation system with prismatic absorber basin: experimental analysis and LSTM machine learning modeling coupled with great wall construction algorithm, Process Saf. Environ. Prot. 186 (2024) 1120–1133, https://doi.org/10.1016/j.psep.2024.04.063.

[38] M. Abd Elaziz, F.A. Essa, A.H. Elsheikh, Utilization of ensemble random vector functional link network for freshwater prediction of active solar stills with nanoparticles, Sustain. Energy Technol. Assessments. 47 (2021) 101405, https://doi.org/10.1016/j.seta.2021.101405.

[39] A.S. Abdullah, F.A. Essa, H. Panchal, W.H. Alawee, A.H. Elsheikh, Enhancing the performance of tubular solar stills for water purification: a comprehensive review and comparative analysis of methodologies and materials, Results Eng 21 (2024) 101722, https://doi.org/10.1016/j.rineng.2023.101722.

[40] F.A. Essa, A.S. Abdullah, Z.M. Omara, Rotating discs solar still: new mechanism of desalination, J. Clean. Prod. 275 (2020) 123200, https://doi.org/10.1016/j.jclepro.2020.123200.

[41] F.A. Essa, Aspects of energy , exergy , economy , and environment for performance evaluation of modified spherical solar still with rotating ball and phase change material, J. Energy Storage. 81 (2024) 110500, https://doi.org/10.1016/j.est.2024.110500.

[42] M. El Hadi Attia, A.K. Hussein, G. Radhakrishnan, S. Vaithilingam, O. Younis, N. Akkurt, Energy, exergy and cost analysis of different hemispherical solar distillers: a comparative study, Sol. Energy Mater. Sol. Cells. 252 (2023) 112187, https://doi.org/10.1016/j.solmat.2023.112187.

[43] A.S. Abdullah, Z.M. Omara, F.A. Essa, U.F. Alqsair, M. Aljaghtham, I.B. Mansir, S. Shanmugan, W.H. Alawee, Enhancing trays solar still performance using wick

finned absorber, nano- enhanced PCM, Alexandria Eng. J. 61 (2022) 12417–12430, https://doi.org/10.1016/j.aej.2022.06.033.
[44] A. Bamasag, F.A. Essa, Z.M. Omara, E. Bahgat, A.O. Alsaiari, H. Abulkhair, R. A. Alsulami, A.H. Elsheikh, Machine learning-based prediction and augmentation of dish solar distiller performance using an innovative convex stepped absorber and phase change material with nanoadditives, Process Saf. Environ. Prot. 162 (2022) 112–123, https://doi.org/10.1016/j.psep.2022.03.052.
[45] B. Saleh, F.A. Essa, A. Aly, M. Alsehli, H. Panchal, A. Afzal, S. Shanmugan, Investigating the performance of dish solar distiller with phase change material mixed with Al2O3 nanoparticles under different water depths, Environ. Sci. Pollut. Res. 29 (2022) 28115–28126, https://doi.org/10.1007/s11356-021-18295-4.
[46] M.R. Diab, F.S. Abou-Taleb, F.A. Essa, Z.M. Omara, Improving the vertical solar distiller performance using rotating wick discs and integrated condenser, Environ. Sci. Pollut. Res. (2022), https://doi.org/10.1007/s11356-022-19873-w.
[47] F.A. Essa, F.S. Abou-Taleb, M.R. Diab, Experimental investigation of vertical solar still with rotating discs, Energy Sources, Part A Recover. Util. Environ. Eff. (2021), https://doi.org/10.1080/15567036.2021.1950238.
[48] F.A. Essa, Z.M. Omara, A.S. Abdullah, S. Shanmugan, H. Panchal, A.E. Kabeel, R. Sathyamurthy, W.H. Alawee, A.M. Manokar, A.H. Elsheikh, Wall-suspended trays inside stepped distiller with Al2O3/paraffin wax mixture and vapor suction: experimental implementation, J. Energy Storage. 32 (2020), https://doi.org/10.1016/j.est.2020.102008.
[49] A.M. Gandhi, S. Shanmugan, S. Gorjian, C.I. Pruncu, S. Sivakumar, A.H. Elsheikh, F.A. Essa, Z.M. Omara, H. Panchal, Performance enhancement of stepped basin solar still based on OSELM with traversal tree for higher energy adaptive control, Desalination 502 (2021) 114926, https://doi.org/10.1016/j.desal.2020.114926.
[50] F.A. Essa, Z. Omara, A. Abdullah, S. Shanmugan, H. Panchal, A.E. Kabeel, R. Sathyamurthy, M.M. Athikesavan, A. Elsheikh, M. Abdelgaied, B. Saleh, Augmenting the productivity of stepped distiller by corrugated and curved liners, CuO/paraffin wax, wick, and vapor suctioning, Environ. Sci. Pollut. Res. 28 (2021) 56955–56965, https://doi.org/10.1007/s11356-021-14669-w.
[51] Z.M. Omara, A.S. Abdullah, F.A. Essa, M.M. Younes, Performance evaluation of a vertical rotating wick solar still, Process Saf. Environ. Prot. 148 (2021) 796–804, https://doi.org/10.1016/j.psep.2021.02.004.
[52] A.K. Hussein, Applications of nanotechnology in renewable energies - a comprehensive overview and understanding, Renew. Sustain. Energy Rev. 42 (2015) 460–476, https://doi.org/10.1016/j.rser.2014.10.027.
[53] A.K. Hussein, F.L. Rashid, M.K. Rasul, A. Basem, O. Younis, R.Z. Homod, M. El Hadi Attia, M.A. Al-Obaidi, M.B. Ben Hamida, B. Ali, S.F. Abdulameer, A review of the application of hybrid nanofluids in solar still energy systems and guidelines for future prospects, Sol. Energy. 272 (2024) 112485, https://doi.org/10.1016/j.solener.2024.112485.
[54] A.S. Abdullah, F.A. Essa, Z.M. Omara, Y. Rashid, L. Hadj-Taieb, G.B. Abdelaziz, A. E. Kabeel, Rotating-drum solar still with enhanced evaporation and condensation techniques: comprehensive study, Energy Convers. Manag. 199 (2019) 112024, https://doi.org/10.1016/j.enconman.2019.112024.
[55] F.A. Essa, A.S. Abdullah, Z.M. Omara, Improving the performance of tubular solar still using rotating drum – experimental and theoretical investigation, Process Saf. Environ. Prot. 148 (2021) 579–589, https://doi.org/10.1016/j.psep.2020.11.039.
[56] A.E. Kabeel, R. Sathyamurthy, A.M. Manokar, S.W. Sharshir, F.A. Essa, A. H. Elshiekh, Experimental study on tubular solar still using Graphene Oxide Nano particles in Phase Change Material (NPCM's) for fresh water production, J. Energy Storage. 28 (2020) 101204, https://doi.org/10.1016/j.est.2020.101204.
[57] F.A. Essa, W.H. Alawee, S.A. Mohammed, H.A. Dhahad, A.S. Abdullah, Z. M. Omara, Experimental investigation of convex tubular solar still performance using wick and nanocomposites, Case Stud. Therm. Eng. 27 (2021) 101368, https://doi.org/10.1016/j.csite.2021.101368.
[58] M.S. El-Sebaey, A. Hegazy, F.A. Essa, Performance enhancement of a tubular solar still by using stepped basins: an experimental approach, J. Clean. Prod. 437 (2024) 140746, https://doi.org/10.1016/j.jclepro.2024.140746.
[59] F.L. Rashid, M.A. Al-Obaidi, A.K. Hussein, N. Akkurt, B. Ali, O. Younis, Floating solar stills and floating solar-driven membranes: recent advances and overview of designs, performance and modern combinations, Sol. Energy. 247 (2022) 355–372, https://doi.org/10.1016/j.solener.2022.10.044.
[60] M.E.H. Attia, A.E. Kabeel, M. Abdelgaied, F.A. Essa, Z.M. Omara, Enhancement of hemispherical solar still productivity using iron, zinc and copper trays, Sol. Energy. 216 (2021) 295–302, https://doi.org/10.1016/j.solener.2021.01.038.
[61] A.E. Kabeel, M. El Hadi Attia, M. Abdelgaied, F.A. Essa, M.F. Aly Aboud, Comparative performance of spherical, hemispherical, and single-sloped solar distillers, Desalin. Water Treat. 317 (2024) 100051, https://doi.org/10.1016/j.dwt.2024.100051.
[62] O. Younis, A.K. Hussein, M.E.H. Attia, F.L. Rashid, L. Kolsi, U. Biswal, A. Abderrahmane, A. Mourad, A. Alazzam, Hemispherical solar still: recent advances and development, Energy Reports 8 (2022) 8236–8258, https://doi.org/10.1016/j.egyr.2022.06.037.
[63] A.K. Hussein, F.L. Rashid, A.M. Abed, M. Al-Khaleel, H. Togun, B. Ali, N. Akkurt, E.H. Malekshah, U. Biswal, M.A. Al-Obaidi, O. Younis, A. Abderrahmane, Inverted solar stills: a comprehensive review of designs, mathematical models, performance, and modern combinations, Sustain 14 (2022) 1–34, https://doi.org/10.3390/su142113766.
[64] Z.M. Omara, W.H. Alawee, S.A. Mohammed, H.A. Dhahad, A.S. Abdullah, F. A. Essa, Experimental study on the performance of pyramid solar still with novel convex and dish absorbers and wick materials, J. Clean. Prod. 373 (2022) 133835, https://doi.org/10.1016/j.jclepro.2022.133835.
[65] W.H. Alawee, A.S. Abdullah, S.A. Mohammed, H.A. Dhahad, Z.M. Omara, F. A. Essa, Augmenting the distillate yield of cords pyramid distiller with baffles within compartments, J. Clean. Prod. 356 (2022) 131761, https://doi.org/10.1016/j.jclepro.2022.131761.
[66] W.M. Farouk, A.S. Abdullah, S.A. Mohammed, W.H. Alawee, Z.M. Omara, F. A. Essa, Modeling and optimization of working conditions of pyramid solar still with different nanoparticles using response surface methodology, Case Stud. Therm. Eng. 33 (2022) 101984, https://doi.org/10.1016/j.csite.2022.101984.
[67] W.H. Alawee, F.A. Essa, S.A. Mohammed, H.A. Dhahad, A.S. Abdullah, Z. M. Omara, Y. Gamiel, Improving the performance of pyramid solar distiller using dangled cords of various wick materials: novel working mechanism of wick, Case Stud. Therm. Eng. 28 (2021) 101550, https://doi.org/10.1016/j.csite.2021.101550.
[68] A.K. Singh, An inclusive study on new conceptual designs of passive solar desalting systems, Heliyon 7 (2021) e05793, https://doi.org/10.1016/j.heliyon.2020.e05793.
[69] A.K. Singh, Analysis for optimized prerequisites of modified solar stills, Heliyon 10 (2024) e25804, https://doi.org/10.1016/j.heliyon.2024.e25804.
[70] Y.A.F. El-Samadony, A.S. Abdullah, Z.M. Omara, Experimental study of stepped solar still integrated with reflectors and external condenser, Exp. Heat Transf. 28 (2015) 392–404, https://doi.org/10.1080/08916152.2014.890964.
[71] M.M. Younes, A.S. Abdullah, F.A. Essa, Z.M. Omara, M.I. Amro, Enhancing the wick solar still performance using half barrel and corrugated absorbers, Process Saf. Environ. Prot. 150 (2021) 440–452, https://doi.org/10.1016/j.psep.2021.04.036.
[72] A.S. Abdullah, W.H. Alawee, S.A. Mohammed, U.F. Alqsair, H.A. Dhahad, F. A. Essa, Z.M. Omara, Performance improvement of tubular solar still via tilting glass cylinder, nano-coating, and nano-PCM: experimental approach, Environ. Sci. Pollut. Res. (2022), https://doi.org/10.1007/s11356-022-20207-z.
[73] A.S. Abdullah, Z.M. Omara, A. Alarjani, F.A. Essa, Experimental investigation of a new design of drum solar still with reflectors under different conditions, Case Stud. Therm. Eng. 24 (2021) 100850, https://doi.org/10.1016/j.csite.2021.100850.
[74] F.A. Essa, W.H. Alawee, S.A. Mohammed, A.S. Abdullah, Z.M. Omara, Enhancement of pyramid solar distiller performance using reflectors, cooling cycle, and dangled cords of wicks, Desalination 506 (2021) 115019, https://doi.org/10.1016/j.desal.2021.115019.
[75] A.S. Abdullah, Z.M. Omara, F.A. Essa, A. Alarjani, I.B. Mansir, M.I. Amro, Enhancing the solar still performance using reflectors and sliding-wick belt, Sol. Energy. 214 (2021) 268–279, https://doi.org/10.1016/j.solener.2020.11.016.
[76] A.K. Singh, Samsher, A review study of solar desalting units with evacuated tube collectors, J. Clean. Prod. 279 (2021) 123542, https://doi.org/10.1016/j.jclepro.2020.123542.
[77] A.K. Singh, S. Gautam, Optimum techno-eco performance requisites for vacuum annulus tube collector–assisted double-slope solar desaltification unit integrated modified parabolic concentrator, Environ. Sci. Pollut. Res. 29 (2022) 34379–34405, https://doi.org/10.1007/s11356-021-18426-x.
[78] A.K. Singh, Mathematical analysis of optimized requisites for novel combination of solar distillers, J. Eng. Res. 11 (2023) 515–525, https://doi.org/10.1016/j.jer.2023.100121.
[79] A.K. Singh, Samsher, Parametric analysis of evacuated annular parabolic solar receiver integrated solar stills: a relative optimization approach, Environ. Dev. Sustain. (2024), https://doi.org/10.1007/s10668-024-04709-z.
[80] L. Hadj-Taieb, S.A. Mohammed, W.H. Alawee, A.S. Abdullah, A. Basem, H. Majdi, Z.M. Omara, F.A. Essa, Enhancing water productivity and cost-effectiveness in hemispherical solar stills using sandy beds, reflectors, and a vapor extraction fan, Results Eng 21 (2024) 101983, https://doi.org/10.1016/j.rineng.2024.101983.
[81] F.A. Essa, A.S. Abdullah, W.H. Alawee, A. Alarjani, U.F. Alqsair, S. Shanmugan, Z. M. Omara, M.M. Younes, Experimental enhancement of tubular solar still performance using rotating cylinder, nanoparticles' coating, parabolic solar concentrator, and phase change material, Case Stud. Therm. Eng. 29 (2022) 101705, https://doi.org/10.1016/j.csite.2021.101705.
[82] M.T. Chaichan, H.A. Kazem, Using aluminium powder with PCM (paraffin wax) to enhance single slope solar water distiller productivity in Baghdad - Iraq winter weathers, Int. J. Renew. Energy Res. 5 (2015) 251–257, https://doi.org/10.20508/ijrer.v5i1.1971.g6492.
[83] H. Panchal, H. Nurdiyanto, K.K. Sadasivuni, S.S. Hishan, F.A. Essa, M. Khalid, S. Dharaskar, S. Shanmugan, Experimental investigation on the yield of solar still using manganese oxide nanoparticles coated absorber, Case Stud. Therm. Eng. 25 (2021) 100905, https://doi.org/10.1016/j.csite.2021.100905.
[84] F.A. Essa, Z.M. Omara, A.S. Abdullah, A.E. Kabeel, G.B. Abdelaziz, Enhancing the solar still performance via rotating wick belt and quantum dots nanofluid, Case Stud. Therm. Eng. 27 (2021) 101222, https://doi.org/10.1016/j.csite.2021.101222.
[85] W. Alawee, S. Mohammed, H.A. Dhahad, A.S. Abdullah, Z.M. Omara, F.A. Essa, Improving the performance of pyramid solar still using rotating four cylinders and three electric heaters, Process Saf. Environ. Prot. 148 (2021) 950–958, https://doi.org/10.1016/j.psep.2021.02.022. (Accessed 10 September 2021).
[86] A.E. Kabeel, Z.M. Omara, F.A. Essa, Numerical investigation of modified solar still using nanofluids and external condenser, J. Taiwan Inst. Chem. Eng. 75 (2017) 77–86, https://doi.org/10.1016/j.jtice.2017.01.017.
[87] A.E. Kabeel, Z.M. Omara, F.A. Essa, Enhancement of modified solar still integrated with external condenser using nanofluids: an experimental approach,

Energy Convers. Manag. 78 (2014) 493–498, https://doi.org/10.1016/j.enconman.2013.11.013.
[88] A.K. Singh, Analysis for modified augmentation of solar desalination assisted water heating system: energy-matrices and environ-economics, Sol. Energy. 285 (2025) 113120, https://doi.org/10.1016/j.solener.2024.113120.
[89] A.K. Singh, Samsher, Techno-environ-economic-energy-exergy-matrices performance analysis of evacuated annulus tube with modified parabolic concentrator assisted single slope solar desalination system, J. Clean. Prod. 332 (2022) 129996, https://doi.org/10.1016/j.jclepro.2021.129996.
[90] L. Malaeb, K. Aboughali, G.M. Ayoub, Modeling of a modified solar still system with enhanced productivity, Sol. Energy. 125 (2016) 360–372, https://doi.org/10.1016/j.solener.2015.12.025.
[91] T. Arunkumar, R. Velraj, D.C. Denkenberger, R. Sathyamurthy, K.V. Kumar, A. Ahsan, Productivity enhancements of compound parabolic concentrator tubular solar stills, Renew. Energy. 88 (2016) 391–400, https://doi.org/10.1016/j.renene.2015.11.051.
[92] T. Arunkumar, A.E. Kabeel, Effect of phase change material on concentric circular tubular solar still-Integration meets enhancement, Desalination 414 (2017) 46–50, https://doi.org/10.1016/j.desal.2017.03.035.
[93] M.T. Chaichan, H.A. Kazem, Water solar distiller productivity enhancement using concentrating solar water heater and phase change material (PCM), Case Stud. Therm. Eng. 5 (2015) 151–159, https://doi.org/10.1016/j.csite.2015.03.009.
[94] M. Elashmawy, Improving the performance of a parabolic concentrator solar tracking-tubular solar still (PCST-TSS) using gravel as a sensible heat storage material, Desalination 473 (2020) 114182, https://doi.org/10.1016/j.desal.2019.114182.
[95] M.A. Al-Nimr, M.E. Dahdolan, Modeling of a novel concentrated solar still enhanced with a porous evaporator and an internal condenser, Sol. Energy. 114 (2015) 8–16, https://doi.org/10.1016/j.solener.2015.01.021.
[96] J.A. Velasco-Parra, F.R. Valencia, A. Lopez-Arraiza, B. Ramón-Valencia, G. Castillo-López, Jute fibre reinforced biocomposite: seawater immersion effects on tensile properties and its application in a ship hull design by finite-element analysis, Ocean Eng 290 (2023) 116301, https://doi.org/10.1016/j.oceaneng.2023.116301.
[97] S. Kim, Y. Cho, C.H. Park, Effect of cotton fabric properties on fiber release and marine biodegradation, Text. Res. J. 92 (2022) 2121–2137, https://doi.org/10.1177/00405175211068781.
[98] R. Rowell, Acetylation of natural fibers to improve performance, Mol. Cryst. Liq. Cryst. - MOL CRYST Liq. CRYST. 418 (2004) 153–164, https://doi.org/10.1080/15421400490479244.
[99] J.P. Holman, Experimental Methods for Engineers, Eighth, McGraw-Hill Companies, New York, 2011.
[100] U.F. Alqsair, A.S. Abdullah, Z.M. Omara, F.A. Essa, Enhanced solar still operation using a copper coil heat exchanger and phase change material integration, J. Energy Storage. 113 (2025), https://doi.org/10.1016/j.est.2025.115557.
[101] F.A. Essa, B. Saleh, A.A. Algethami, S.O. Oyedepo, Z.M. Omara, M.S. El-Sebaey, Enhanced solar desalination via hemispheric distiller with thermal storage, heaters, and condensation: exergoeconomic and environmental analysis, Sol. Energy Mater. Sol. Cells. 285 (2025) 113529, https://doi.org/10.1016/j.solmat.2025.113529.
[102] G.N. Tiwari, Lovedeep sahota, advanced solar-distillation systems: basic principles, thermal modeling, and its application, 2017, https://doi.org/10.1007/978-981-10-4672-8.
[103] O. Bait, Exergy, environ–economic and economic analyses of a tubular solar water heater assisted solar still, J. Clean. Prod. 212 (2019) 630–646, https://doi.org/10.1016/j.jclepro.2018.12.015.
[104] S.A. Mousavi, M. Mehrpooya, A comprehensive exergy-based evaluation on cascade absorption-compression refrigeration system for low temperature applications - exergy, exergoeconomic, and exergoenvironmental assessments, J. Clean. Prod. 246 (2020) 119005, https://doi.org/10.1016/j.jclepro.2019.119005.
[105] S.M. Parsa, A. Yazdani, H. Dhahad, W.H. Alawee, S. Hesabi, F. Norozpour, D. Javadi Y, H.M. Ali, M. Afrand, Effect of Ag, Au, TiO2 metallic/metal oxide nanoparticles in double-slope solar stills via thermodynamic and environmental analysis, J. Clean. Prod. 311 (2021) 127689, https://doi.org/10.1016/j.jclepro.2021.127689.
[106] G. Kopp, J.L. Lean, A new, lower value of total solar irradiance: evidence and climate significance, Geophys. Res. Lett. 38 (2011), https://doi.org/10.1029/2010GL045777.
[107] Y. Yin, C. Guo, Q. Mu, W. Li, H. Yang, Y. He, Dual-sensing nano-yarns for real-time pH and temperature monitoring in smart textiles, Chem. Eng. J. 500 (2024) 157115, https://doi.org/10.1016/j.cej.2024.157115.
[108] A. Ali, K. Shaker, Y. Nawab, M. Ashraf, A. Basit, S. Shahid, M. Umair, Impact of hydrophobic treatment of jute on moisture regain and mechanical properties of composite material, J. Reinf. Plast. Compos. 34 (2015) 2059–2068, https://doi.org/10.1177/0731684415610007.
[109] K.M. Kuroki Iwasaki, R. Medeiros, D. Becker, Thermal and Mechanical Properties of Jute Fiber, 2021.
[110] N. Dai, L. Li, K. Xu, Z. Lu, X. Hu, Y. Yuan, Development of a standardized data collection and intelligent fabric quality prediction system for the weaving department, J. Eng. Fibers Fabr. . 20 (2025), https://doi.org/10.1177/15589250241312778/ASSET/DAEB202D-5037-4EB4-BDE8-01B9750B8300/ASSETS/IMAGES/LARGE/10.1177_15589250241312778-FIG14.JPG.
[111] S. Hosseini, J.F. Torres, M. Taheri, A. Tricoli, W. Lipiński, J. Coventry, Long-term thermal stability and failure mechanisms of Pyromark 2500 for high-temperature solar thermal receivers, Sol. Energy Mater. Sol. Cells. 246 (2022) 111898, https://doi.org/10.1016/j.solmat.2022.111898.
[112] C. Okorieimoh, B. Norton, M. Conlon, LONG-TERM DURABILITY OF SOLAR PHOTOVOLTAIC MODULES, 2019.
[113] H. Liu, D. Ji, M. An, A.W. Kandeal, A. Kumar, M.R. Elkadeem, A.M. Algazzar, G. B. Abdelaziz, S.W. Sharshir, Performance enhancement of solar desalination using evacuated tubes , ultrasonic atomizers , and cobalt oxide nanofluid integrated with cover cooling, Process Saf. Environ. Prot. 171 (2023) 98–108, https://doi.org/10.1016/j.psep.2023.01.009.
[114] W.H. Alawee, S.A. Mohammed, A.S. Abdullah, A. Basem, A.D.J. Al-Bayati, Z. M. Omara, F.A. Essa, Utilizing the dangled jute cords, reflectors, and condensation cycle to improve the double sloped distiller performance, Sol. Energy. 267 (2024) 112237, https://doi.org/10.1016/j.solener.2023.112237.
[115] M.M.Z. Ahmed, F. Alshammari, A.S. Abdullah, M. Elashmawy, Enhancing tubular solar still performance using double effect with direct sunrays concentration, Sol. Energy Mater. Sol. Cells. 230 (2021) 111214, https://doi.org/10.1016/j.solmat.2021.111214.
[116] M. Abdelgaied, Y. Zakaria, A.E. Kabeel, F.A. Essa, Improving the tubular solar still performance using square and circular hollow fins with phase change materials, J. Energy Storage. 38 (2021) 102564, https://doi.org/10.1016/j.est.2021.102564.
[117] R. Sathyamurthy, D. Mageshbabu, B. Madhu, A. Muthu Manokar, A. Rajendra Prasad, M. Sudhakar, Influence of fins on the absorber plate of tubular solar still-an experimental study, Mater. Today Proc. 46 (2020) 3270–3274, https://doi.org/10.1016/j.matpr.2020.11.355.
[118] F. Alshammari, M. Elashmawy, M.M.Z. Ahmed, Cleaner production of freshwater using multi-effect tubular solar still, J. Clean. Prod. 281 (2021) 125301, https://doi.org/10.1016/j.jclepro.2020.125301.
[119] T. Yan, G. Xie, W. Chen, Z. Wu, J. Xu, Y. Liu, Experimental study on three-effect tubular solar still under vacuum and immersion cooling, Desalination 515 (2021) 115211, https://doi.org/10.1016/j.desal.2021.115211.